Original Contribution

UV irradiation-induced zinc dissociation from commercial zinc oxide sunscreen and its action in human epidermal keratinocytes

Lisa M Martorano, DO Candidate,[1*] Christian J Stork, PhD Candidate,[2*] & Yang V Li, MD, PhD[1,2,3]

[1]*Ohio University College of Osteopathic Medicine, Ohio University, Athens, Ohio, USA*
[2]*Molecular and Cellular Biology Graduate Program, Ohio University, Athens, Ohio, USA*
[3]*Department of Biomedical Sciences, Ohio University, Athens, Ohio, USA*
**These authors contributed equally*

Summary

Zinc oxide (ZnO) is an active ingredient in sunscreen owing to its properties of broadly filtering the ultraviolet (UV) light spectrum and it is used to protect against the carcinogenic and photodamaging effects of solar radiation on the skin. This study investigated the dissociation of zinc (Zn^{2+}) from ZnO in commercial sunscreens under ultraviolet type B light (UVB) irradiation and assessed the cytotoxicity of Zn^{2+} accumulation in human epidermal keratinocytes (HEK). Using Zn^{2+} fluorescent microscopy, we observed a significant increase in Zn^{2+} when ZnO sunscreens were irradiated by UVB light. The amount of Zn^{2+} increase was dependent on both the irradiation intensity as well as on the ZnO concentration. A reduction in cell viability as a function of ZnO concentration was observed with cytotoxic assays. In a real-time cytotoxicity assay using propidium iodide, the treatment of UVB-irradiated ZnO sunscreen caused a late- or delayed-type cytotoxicity in HEK. The addition of a Zn^{2+} chelator provided a protective effect against cellular death in all assays. Furthermore, Zn^{2+} was found to induce the production of reactive oxygen species (ROS) in HEK. Our data suggest that UVB irradiation produces an increase in Zn^{2+} dissociation in ZnO sunscreen and, consequently, the accumulation of free or labile Zn^{2+} from sunscreen causes cytotoxicity and oxidative stress.

Keywords: sunscreens, UV damage, zinc

Introduction

Prolonged human exposure to solar ultraviolet (UV) radiation results in sunburn and increases the potential for carcinogenicity and premature aging effects on the skin.[1–4] As an FDA-approved active ingredient in sunscreen,[5] ZnO offers superior protection for human skin against the full spectrum of ultraviolet light, including UVA1, UVA2, as well as ultraviolet type B light (UVB) wavelengths. However, little is known about the potential long-term effects of their usage. Sunscreen use itself may be associated with adverse effects.[6] In particular, some sunscreen ingredients such as metal oxides may be associated with the generation of harmful reactive oxygen species (ROS) in skin.[7,8]

The cytotoxic effect of ZnO and its ability to induce cell apoptosis have been studied in a variety of cell types.[9–16] It has been speculated that the mechanism of ZnO-induced cytotoxicity involves the production of ROS, which contributes to the apoptotic effect of ZnO.[17] Additionally, the cytotoxic effect of Zn^{2+} is also reported in other zinc compounds such as $ZnCl_2$. Once dissociated

Correspondence: Yang V Li, MD, PhD, Department of Biomedical Sciences, 346 Irvine Hall, Athens, OH 45701, USA. E-mail: li@oucom.ohiou.edu

Accepted for publication July 11, 2010

from its parent compound, the rise of intracellular Zn^{2+} was shown to disrupt mitochondrial function and induce the apoptotic pathway at lower concentrations, while resulting in cellular necrosis at higher concentrations.[17–24]

There is considerable concern as to the stability of ZnO under UV irradiation.[17,25–29] Under UV irradiation, the concentration of Zn^{2+} ions in solution resulting from the photodecomposition of ZnO increases with increasing doses of irradiation.[30] Thus, UV irradiation facilitates photodecomposition or photoreaction throughout the duration of sunscreen use. However, there is little information available regarding the effects of irradiation on Zn^{2+} dissociation in ZnO sunscreen, and to date there is no information about the cytotoxic effect of dissociated Zn^{2+} in ZnO-containing sunscreens. The purpose of this study was therefore to investigate the Zn^{2+} dissociation in ZnO sunscreen upon UVB irradiation. The amount of Zn^{2+} release was characterized with fluorescent Zn^{2+} indicators using fluorescent microscopy. In addition, the cytotoxicity of the released Zn^{2+} in human epidermal keratinocytes (HEK) and the generation of ROS were also studied.

Materials and methods

Materials

Tetrakis-(2-pyridylmethyl)ethylenediamine (TPEN), Newport Green, 3-(4,5-dimethylthiazol-2-yl)-2,5-diphenyltetrazolium bromide (MTT), propidium iodide, and MitoSOX (red mitochondrial superoxide indicator) were purchased from Invitrogen (Carlsbad, CA, USA). Pyrithione (1-hydroxy-2-pyridinethione sodium salt), ZnO, 2′,7′-dichlorofluorescein diacetate (DCFH-DA), and buffer salts were purchased from Sigma-Aldrich (St Louis, MO, USA).

Sunscreen solution

Sunscreen from commercial samples (0.5 mL) was dissolved in 20 mL of pure acetone and stirred at 37 °C for 1 h to attain 21 mM ZnO in each sample. The ZnO concentration was determined from a proportion such that 6.86%g ZnO/100 mL of sample approximates 840 mM and 0.5 mL thus equates to 21 mM or 0.2%g ZnO/100 mL sunscreen. From the aqueous stock solution, the sunscreen solutions were diluted further in the following (in mM): 130 NaCl, 5 KCl, 8 $MgSO_4$, 1 Na_2HPO_4, 25 glucose, 20 HEPES, 1 Na-pyruvate; pH adjusted to 7.4 (1X HEPES medium) to obtain the final concentrations of ZnO (1, 10, and100 μM) (w/v%) in sunscreen (aqueous), respectively. All sunscreen preparations were stored at room temperature and away from light.

Fluorescence microscopy

UV Radiation

Ultraviolet type B light dosages were chosen such that 100 mJ/cm^2 is equivalent to five minimal erythemal dosages (MEDs) and 1000 mJ/cm^2 is equivalent to 50 MEDs for skin type II, respectively.[31] A single UVB wavelength source (8 W, 3 UV™ lamp, UVP, Upland, CA, USA) of 302 nm was applied throughout the experiment. The UV light source was suspended above the stage to avoid potential contacts with the recording stage. This arrangement of experimental setup avoided potential artifacts by motion and enabled continuous fluorescence acquisition before and after the irradiation.

Intracellular Free Zn^{2+} Measurement

The aqueous sunscreen solutions containing the desired ZnO concentrations in HEPES medium were transferred to 35-mm glass bottom petri dishes and mounted on the stage of a fluorescence microscope prior to UV irradiation. Newport Green (10 μM), a derivative of a metal ion chelator, was added to each petri dish to detect changes in fluorescence. TPEN was then added to the medium to chelate any remaining zinc and confirmed the presence of Zn^{2+}. Fluorescence was monitored using a customer-designed inverted fluorescence microscope equipped with a mercury lamp light source in addition to a 488/15 nm BP filter for excitation and a 530 nm LP emission filter. Images were processed and analyzed using Image-Pro (Media Cybernetics, Silver Spring, MD, USA) or NIH ImageJ software (NIH, Bethesda, MD, USA).

HEK culture

Human epidermal keratinocytes cells and growth medium were purchased from Invitrogen (Carlsbad, CA, USA) and seeded into collagen coated 24 well-plates or 35 mm glass bottom petri dishes. For UV irradiation experiments, direct UVB irradiation of cultured HEK cells was employed as follows. Cells grown in 35 mm glass bottom petri dishes were mounted on the stage of a fluorescence microscope with a UV-light source as stated above. UVB intensity in this experimental setup was monitored (average UVB intensity = 7 mW/cm^2) and UVB exposure times were employed so as to achieve the UVB dosages indicated in the text.

Viability assays

Cytotoxicity (MTT assay)

The MTT assay is based on the production of purple formazan pigment from methyltetrazolium salt by the

mitochondrial enzymes of viable cells, and is sensitive to the function of labile mitochondrial enzymes, which typically lose activity early in the progression towards death. After exposure to the indicated experimental treatments, the viability of HEK cells grown in 24-well plates was analyzed by MTT assay. Cells were rinsed three times with HEPES, equilibrated for 30 min at 37 °C, then were incubated for 4 hours at 37 °C in HEPES containing MTT at a concentration of 1 mg/mL. Following incubation the MTT solution was aspirated, wells were rinsed three times with PBS, and the deposited formazan crystals were solubilized in DMSO. The absorbance of the MTT was measured at 570 nm using a BioMate 3 spectrophotometer (Thermo Scientific, Rochester, NY, USA).

Propidium Iodide (PI) assay

Propidium iodide is excluded from entering the lipid bilayer because of the molecule's size and charge, but in nonviable cells, the dye freely enters the damaged membrane to bind nucleic acids (DNA and RNA) and yields bright red fluorescence. In this study, PI was used at a final concentration of 10 μg/mL in HEPES medium containing the desired ZnO treatment. PI uptake was monitored using a 543/20 nm BP excitation filter and a 580 nm LP emission filter.

ROS detection

Reactive oxygen species/superoxide formation in mitochondria was assessed using MitoSOX (Invitrogen, Carlsbad, CA, USA), which is live-cell permeant and is selectively targeted to the mitochondria. Once in the mitochondria, MitoSOX Red reagent is oxidized by superoxide and exhibits bright red fluorescence on binding to nucleic acids. The intracellular levels of ROS were also measured with DCFH-DA. DCFH-DA is cleaved intracellularly by nonspecific esterases to form DCFH, which is further oxidized by ROS to form the fluorescent compound DCF. In this experiment, HEK cells were treated with ZnO (10 μM) in which the subsequent increase in intracellular Zn^{2+} was facilitated by co-application of the Zn^{2+} ionophore pyrithione (10 μM). The generation of ROS was then measured with MITOSOX and DCF, respectively, and analyzed using Image Pro software. Furthermore, the addition of H_2O_2 (1 mM) to the medium acted as a positive control for comparison of ROS generation.

Results

We tested three commercially available sunscreens: Sunscreen A, B, and C. The table in Figure 1a lists the amount of ZnO in each of the commercial products. Sunscreens A and B contain ZnO, 10% and 6% w/v%, respectively, as an active ingredient to prevent sunburn. Sunscreen A is listed as a sunscreen, B is listed as a skin care lotion, and C is a non-ZnO sunscreen formulation. Sunscreens A and B contain only ZnO UV filters while sunscreen C contains the organic UV filters: padimate O, oxybenzone, and octyl methoxycinnamate. There appears to be a significant amount of free Zn^{2+} in sunscreens. When measured with a fluorescent Zn^{2+} indicator, the addition of sunscreen induced the concentration-dependent increases in Zn^{2+} fluorescence (Fig. 1b,c), suggesting the presence of some basal free Zn^{2+} that may be because of Zn^{2+} contamination or dissociated Zn^{2+} from ZnO sunscreen in its aqueous condition. The amount of basal Zn^{2+} is estimated to be <1 μM (see Fig. 3).

UVB-induced Zn^{2+} releases from ZnO sunscreens

The amount of Zn^{2+} released from ZnO sunscreen solutions during UVB irradiation was studied. When measured with a fluorescent Zn^{2+} indicator, there were significant increases of Zn^{2+} in the sunscreen solutions immediately after the irradiation (Fig. 2a). The increase in zinc induced by UVB irradiation was further confirmed when it was reduced by the addition of the Zn^{2+} chelator, TPEN. Increases in Zn^{2+} concentration were seen neither in the vehicle control (medium without sunscreen) nor in sunscreen C, the non-ZnO formulation. The amount of Zn^{2+} dissociated in the sunscreen solutions was UVB dose-dependent. Longer duration of irradiation (Fig. 2b), as well as stronger intensity of irradiation (Fig. 2c), yielded higher Zn^{2+} concentration. The rising UVB-induced Zn^{2+} release was also sunscreen concentration-dependent (Fig. 2d). The nonlinearity of Zn^{2+} fluorescence observed at the high UVB irradiation suggests the photobleaching of the indicator, which is possibly caused by the fluorescence saturation at greater levels of sunscreen (500 μM) such that the indicator can no longer detect rising Zn^{2+} levels.

The approximate concentration of Zn^{2+} released from ZnO sunscreen under UVB irradiation was calculated using the following formula:[32] $[Zn^{2+}] = K_D\ (F - F_{min})/(F_{max} - F)$, where F is the measured fluorescence intensity. F_{min} and F_{max} are fluorescence with no Zn^{2+} and saturating Zn^{2+}, respectively, and K_D is the dissociation constant (1 μM for Newport Green). F_{min} was obtained by the application of Zn^{2+} chelator TPEN, and F_{max} was obtained by the application of 300 μM $ZnCl_2$ (Fig. 3). We intended to estimate Zn^{2+} concentration released for 10 and 100 μM ZnO sunscreens. However,

a.

	Sunscreen A	Sunscreen B	Sunscreen C
ZnO conc. v%	10%	6%	0%

b.

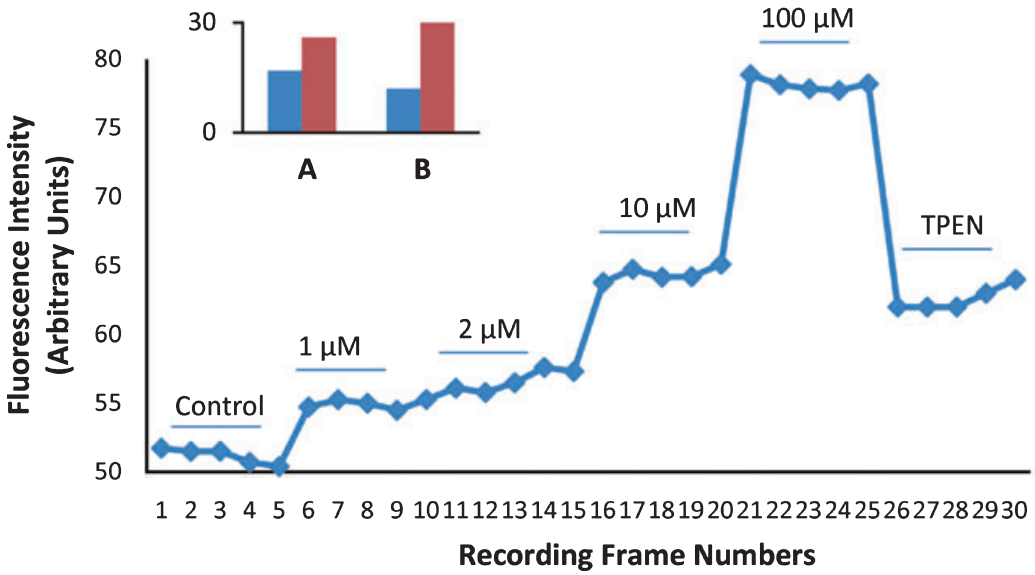

Figure 1 Basal free Zn^{2+} in ZnO sunscreens. (a) Table lists ZnO content in three tested sunscreens. (b) A line graph shows the sunscreen concentration-dependent increases in zinc fluorescence measured with selective fluorescent Zn^{2+} indicator Newport Green. The applied sunscreen Zn^{2+} concentrations were 1, 2, 10, and 100 μM. Zinc chelator TPEN (10 μM) reduced the zinc fluorescence. *Insert*, a histogram summarizes the increases in zinc fluorescence induced by 10 or 100 μM sunscreen zinc in sunscreens A and B (n = 5).

the application of 1000 mJ/cm^2 irradiation to 100 μM ZnO sunscreen solution reached the maximum fluorescence, indicating that the amount of Zn^{2+} might be outside the range of fluorescence detection by Newport Green. Therefore, it was impossible to calculate the concentration of Zn^{2+} released from 100 μM ZnO sunscreens. The concentration of Zn^{2+} released from 10 μM ZnO sunscreen was estimated to be 2–4 μM (Fig. 3c).

Cytotoxicity induced by ZnO (Cytotoxicity of ZnO)

Because the active ingredient in sunscreens is ZnO, we tested HEK viability with an MTT assay in the presence of ZnO. ZnO is minimally soluble in water, and the maximum amount of soluble Zn^{2+} is 50 μM (based on 5 mg/L solubility at 25 °C).[33,34] When HEK were treated for 1 hour with 10 μM or 50 μM ZnO (not ZnO sunscreen), there was a significant and concentration-dependent reduction in cell viability (Fig. 4a). The concentrations of ZnO applied are equivalent to the amount of ZnO that are soluble in water. The percentage of MTT reduction at 10 μM was 60%, and 80% at 50 μM, indicating that rational amounts of soluble ZnO produced marked HEK death. The cytotoxic effect of ZnO was completely prevented by the addition of the Zn^{2+} chelator CaEDTA (Fig. 4b).

Zn^{2+} induced oxidative stress

To identify the mechanisms of cell death caused by zinc, we explored whether the application of Zn^{2+} could induce the generation of hydrogen peroxide (H_2O_2) or ROS, both of which make an important contribution to UV-mediated cell death. In this set of experiments, UV irradiation was not applied so that the generation of ROS was attributed to the application of Zn^{2+} and its subsequent entry into cells. To facilitate Zn^{2+} entry, the Zn^{2+} ionophore, Na-pyrithione, was co-applied in the tests. It is noted that transdermal penetration

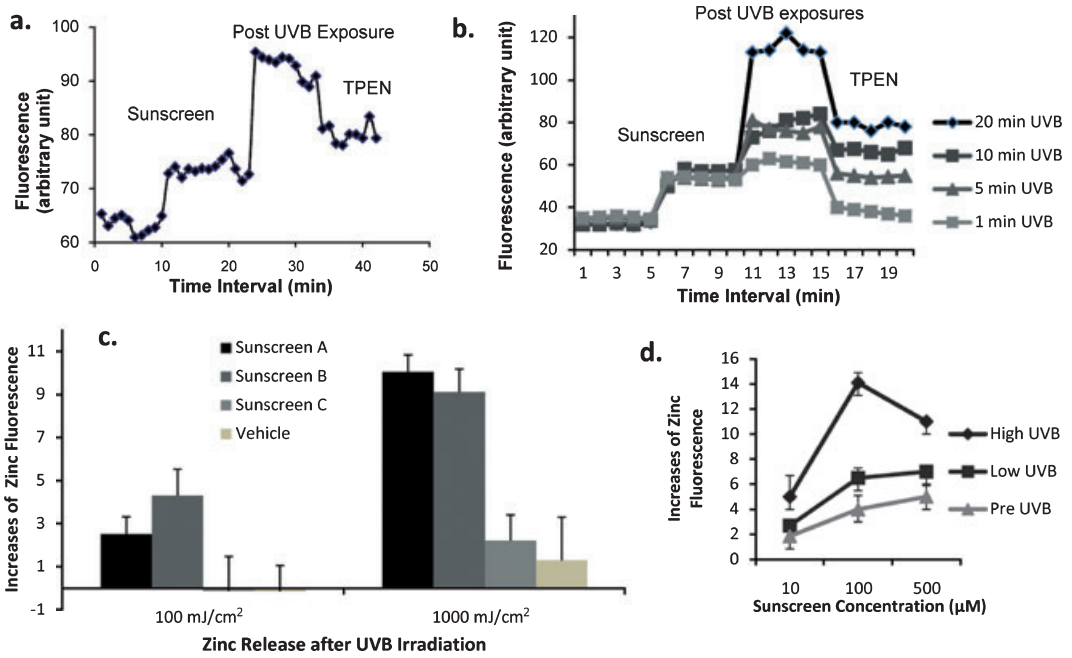

Figure 2 Zn^{2+} releases from ZnO sunscreen under UVB irradiation. (a) A line graph shows the increase in Zn^{2+} in UVB-irradiated ZnO sunscreen (100 μM). Zinc was measured immediately, using fluorescent Zn^{2+} indicator Newport Green, after the irradiation. The addition of Zn^{2+} chelator TPEN (10 μM) reduced the level of Zn^{2+} concentration. (b) Line graphs show UVB dose (irradiation duration)-dependent zinc increase. The test was carried out similar to A but with the irradiation duration ranges of 1, 5, 10, and 20 min. (c) Histograms summarize the UVB-induced Zn^{2+} releases in sunscreen A, B, C, and vehicle (medium without sunscreen) in low (100 mJ/cm^2) or high (1000 mJ/cm^2) UVB irradiation. (d) Line graphs show the sunscreen dose-dependent increase in Zn after UVB irradiation (1000 mJ/cm^2).

enhancers such as HPE-101 (1-[2-(decylthio)ethyl]aza-cyclopentan-2-one) are commonly found in skin care products. In response to the application of Zn^{2+}, the rate of oxidant or ROS generation, detected by MitoSOX or DCF, respectively, increased immediately (Fig. 4c,d).

Late cytotoxic effect of ZnO sunscreen and alleviation (reduction) by Zn^{2+} chelator

The possibility of a delayed or late cytotoxic effect of Zn^{2+} released from sunscreen after UVB irradiation on skin cells was investigated with HEK while the cells were co-cultured with ZnO sunscreen. Cytotoxicity was tested with a PI assay to attain essentially a real-time measurement of the percentage of dead cells in this experiment. The culture medium containing ZnO sunscreen (1 mM) was irradiated with UVB. As we did not intend to irradiate HEK directly, the sunscreen medium was irradiated separately. This medium then replaced the medium in HEK. The final concentration was somewhat less than 1 mM (≈500 μM) because of the inability to air dry the cells. After transferring Zn^{2+} sunscreen solution to the cell cultures dishes, the PI staining or PI-positive cells were measured continuously under fluorescent microscopy every half hour (30 min) for 5 h. The cells were then lysed with Triton X-100 to obtain the total cell counts in each of the cultures. There was no increase in PI staining over time in the control. Figure 5 shows cellular viability over time. In cell cultures treated with ZnO sunscreen, there were significant increases in PI positive-staining cells or dead cells; however, the marked increase did not result until several hours after applying the ZnO sunscreen solution (Fig. 5). Compared to cells treated with the sunscreen media alone, the marked increases in dead cells were observed significantly sooner (2 h) and higher (60%) when HEK were treated with UVB-irradiated sunscreens.

Because UVB exposures resulted in increased levels of free zinc released from ZnO sunscreen and ZnO exerted cytotoxicity as shown above, we wished to determine whether this cytotoxic effect of the sunscreens was involved with intracellular Zn^{2+}. We utilized the Zn^{2+} chelator CaEDTA (1 mM) and mixed it along with the ZnO sunscreen solution. The administration of Zn^{2+} chelator to ZnO sunscreen significantly reduced HEK death compared to cell death in the sunscreen-only HEK group (Fig. 6).

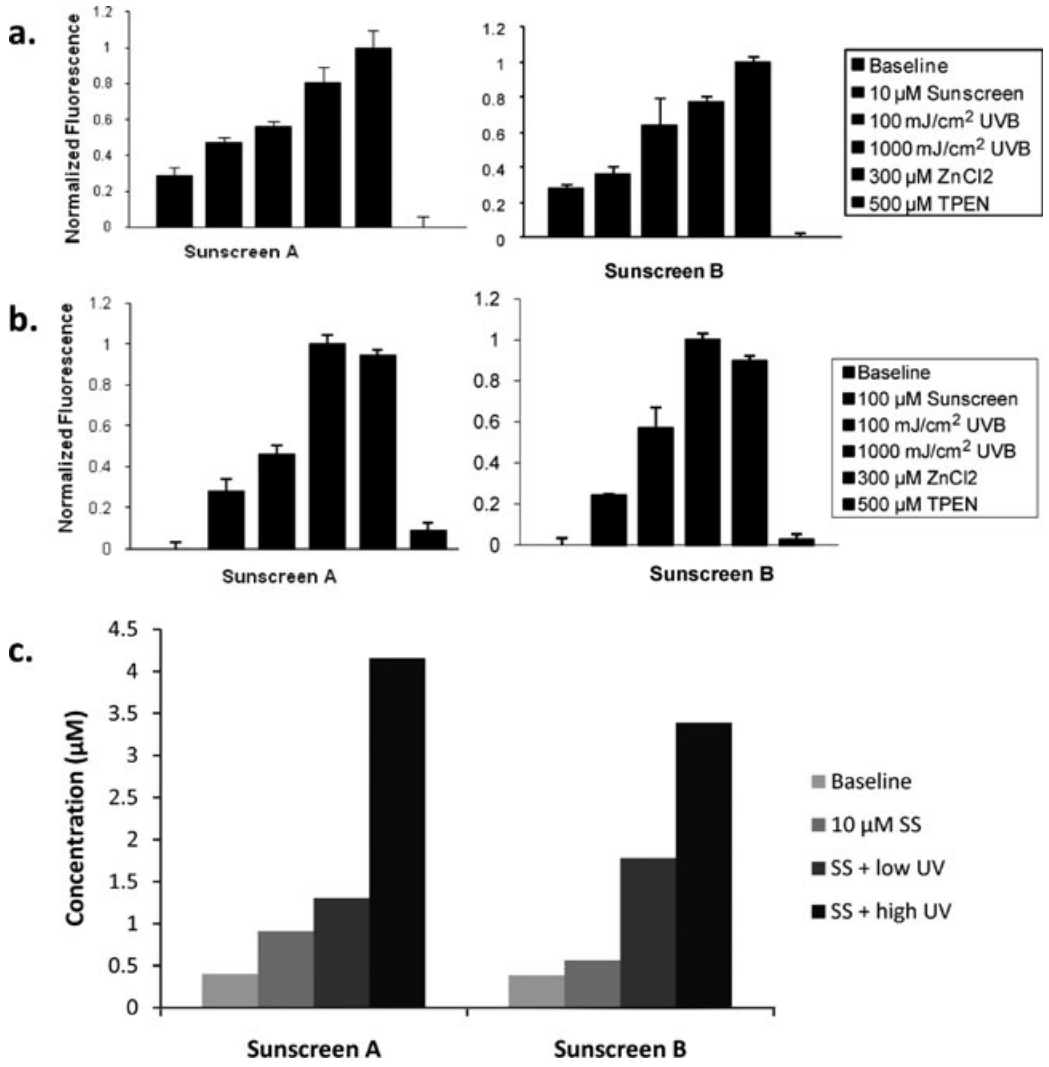

Figure 3 Zn^{2+} concentration measured with fluorescent Zn^{2+} indicator, Newport Green, after UVB irradiation. (a, b) The change of zinc fluorescence as measured in the following sequences: control, the addition of sunscreen (10 or 100 μM), low (100 mJ/cm^2) and high (1000 mJ/cm^2) UVB irradiations, the addition of 300 μM $ZnCl_2$, and the addition of 500 μM TPEN. The changes of fluorescence were normalized to ($F_{max} - F_{min}$). Histograms in a show the fluorescence in 10 μM ZnO sunscreens, where F_{max} is by 300 μM $ZnCl_2$, and F_{min} is by 500 μM TPEN. The application was applied to 100 μM ZnO sunscreen in histogram b. The addition of TPEN did not quench Zn^{2+} fluorescence completely in b. (c) Concentrations of Zn^{2+} in 10 μM ZnO sunscreens (Sunscreen A and Sunscreen B) after UVB irradiation. SS, sunscreen.

Discussion

The major finding in this study suggests that UVB irradiation produces an increase in Zn^{2+} dissociation in ZnO sunscreen and, consequently, the accumulation of free or labile Zn^{2+} in sunscreen causes late cytotoxicity and oxidative stress. There is a noticeable amount of basal Zn^{2+} in the sunscreen mixture. Specifically, we observed a significant increase in Zn^{2+} concentration when ZnO sunscreens were irradiated by UVB light. Increases in Zn^{2+} were not seen in the vehicle control and non-ZnO sunscreen formulation. The increases were dependent on UVB irradiation intensity and exposure time. While ZnO significantly reduced the viability of HEK, we observed that ZnO sunscreens, after UVB irradiation, caused late cytotoxicity of HEK. There were Zn^{2+}-induced cytosol and mitochondrial ROS formation in HEK culture. Taken together, our data suggest that Zn^{2+} dissociation in ZnO products, even at low concentration, possesses a cytotoxic potential in HEK, which may be mediated through oxidative stress.

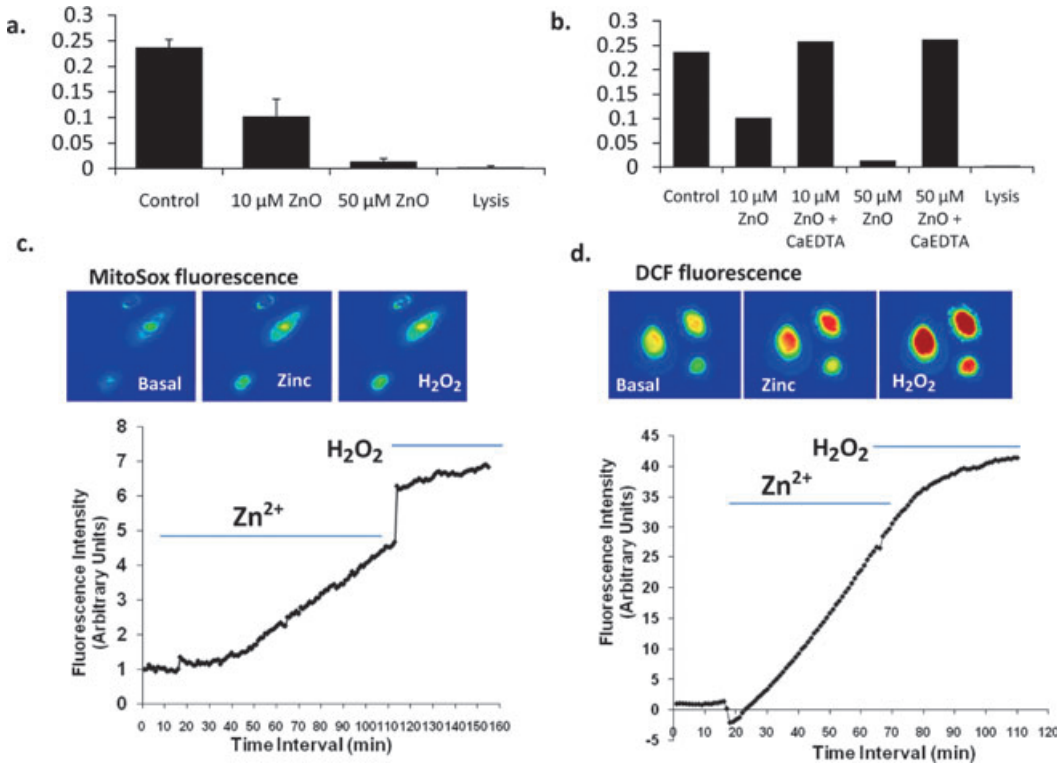

Figure 4 Reduction in human epidermal keratinocytes (HEK) viability and oxidant formation in HEK by Zn^{2+} application. (a) The histogram shows MTT reduction after ZnO exposure (10 or 50 μM) for 1 h in MTT assay. (b) The histogram shows that Zn^{2+} chelator, CaEDTA (1 mM), prevented HEK from the toxic effect of ZnO measured in MTT assay. Values are means ± SEM n = 3 or 4. ZnO was dissolved in HEPES (1X); therefore, controls were HEPE (1X). Total cell death was induced by lysis with 1% (v/v) Triton X-100, as a negative control. (c) A line graph and fluorescent images show the increases in mitochondrial superoxide/reactive oxygen species (ROS) detected by MitoSOX in the presence of ZnO (10 μM) and its ionophore pyrithione (10 μM). (d) A line graph and images show the increase in intracellular ROS production detected by DCF fluorescence in the presence of ZnO (10 μM) and its ionophore pyrithione (10 μM). The ROS productions produced by the application of H_2O_2 provided positive controls in both measurements.

ZnO is a major ingredient in cosmetics and sunscreens.[35] The maximum allowable concentration of ZnO sunscreen is 25%,[5] although the commercial sunscreen of the highest ZnO content we found is 10% (Sunscreen A in this study). The basal Zn^{2+} concentration (Fig. 1) may be the result of spontaneous ZnO decomposition or a contamination Zn^{2+} source during preparation of the sunscreen. The stability of ZnO can be affected by factors such as aqueous environment, pH, or hydroxyl radicals, and there are concerns about the instability of ZnO particles in aqueous solution.[30,36,37] In recent years, nano-ZnO is widely applied in cosmetics including sunscreens. When nano-ZnO is immersed in water, the solubility may be affected by the increased surface of nano-ZnO in equilibrium with Zn^{2+} dissociation.[15] The solubility of those nanoparticles strongly influenced their cytotoxicity.[9,38,39]

To the best of our knowledge, Zn^{2+} dissociation in ZnO sunscreen solution has not been reported. When ZnO sunscreen solution was irradiated with UVB, we observed significant increases in Zn^{2+} concentration, which were dependent on exposure time and dose (Fig. 2). In the tested sunscreen solution, the amount of Zn^{2+} dissociated under strong (1000 mJ/cm^2) UV irradiation is about 1/3 of the total ZnO sunscreen (10 μM) (Fig. 3). How much Zn^{2+} actually becomes available in higher concentrations of ZnO sunscreen application (e.g. 100 μM) remains to be determined, because the increase in fluorescence intensity after UV irradiation was outside the range of detection. Generally, a fluorescent indicator can measure concentrations of its target up to 1 order of its K_D. The K_D of Newport Green for Zn^{2+} is about 1–3 μM.[40] It has been shown that under UV irradiation the concentration of Zn^{2+} ions in aqueous condition resulting from the ZnO photodecomposition increases with increasing dose of irradiation.[30] The results of the present study demonstrate a substantial amount of Zn^{2+} dissociation from ZnO sunscreen under UV irradiation.

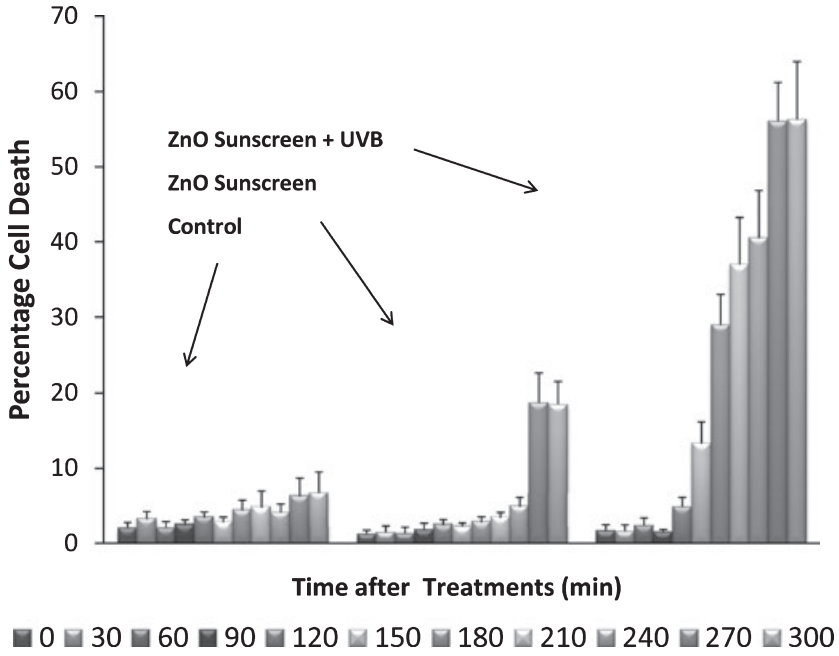

Figure 5 Real-time analysis of dead cells (human epidermal keratinocytes [HEK]) treated with ZnO sunscreen using propidium iodide assay. The histogram shows the percentage of HEK death in three conditions: vehicle control, ZnO sunscreen without pre-UVB irradiation, and ZnO sunscreen with pre-UVB irradiation. The % is calculated to the maximum number of dead cells counted after lysis by triton X-100. The samples were measured every 30 min.

Therefore, it is reasonable to speculate that UV irradiation facilitates ZnO photodecomposition or photoreaction throughout the duration of sunscreen use. In addition, it is important to note that using a single-wavelength source of 302 nm may have impacted the level of Zn^{2+} release seen in the present study. Future studies should incorporate the use of multiple wavelengths that reflect the wide range of UV rays sunscreen users are exposed to on a daily basis to accurately reflect free Zn^{2+} release.

The cytotoxic effect of Zn^{2+} observed in this study is consistent with many studies that show ZnO exerts a cytotoxic effect and induces cell apoptosis in a variety of cell types.[9–16] Although a considerably low concentration of ZnO was applied, the addition of ZnO produced significant cytotoxic effects. The addition of 10 μM (or 0.81 mg/L) and 50 μM (or 4.05 mg/L) ZnO produced 30% and 80% HEK death, respectively, in the MTT assay. The toxological properties of ZnO are determined by its water solubility and persistence.[39,41,42]

Treatment of HEK with ZnO sunscreen also caused cytotoxicity and cell death. However, significant increases in cell death did not occur until several hours after application of sunscreen treatments in a real-time cytotoxicity assay (Fig. 5), indicating a late cytotoxic effect of ZnO sunscreen application. This is consistent with the common warning that prolonged application of sunscreen may actually cause injury to the skin.[6] Significantly, the UVB-irradiated sunscreen induced a much earlier and significantly more (60%) cell death compared to the amount of cell death induced by the same sunscreen preparation without the presence of UV irradiation (Figs 5 and 6). Furthermore, we show that the Zn^{2+} chelator, CaEDTA, completely reversed the cytotoxic action of ZnO and significantly reduced the cytotoxic effect of UV-irradiated ZnO sunscreen (Figs 4b and 6).

The application of Zn^{2+} on HEK cultures resulted in the formation of ROS (Fig. 4c,d), suggesting the attribution of oxidative stress to the cytotoxicity of Zn^{2+} observed in this study. The mechanism of ZnO-induced cytotoxicity involves the production of ROS contributing to the apoptotic effect of Zn^{2+}.[43–48] Several studies recently suggest that Zn^{2+} induces neuronal death by injury to the mitochondria.[49–53] Thus, Zn^{2+} may lead to uncoupling of oxidative phosphorylation and accumulation of ROS in the mitochondria. The interaction between Zn^{2+} and some of the downstream signaling molecules such as 12-LOX, ERK1/2, or p38 MAPK was reported recently.[54] A recent study suggests that acute exposure of ZnO significantly upregulates mRNA levels

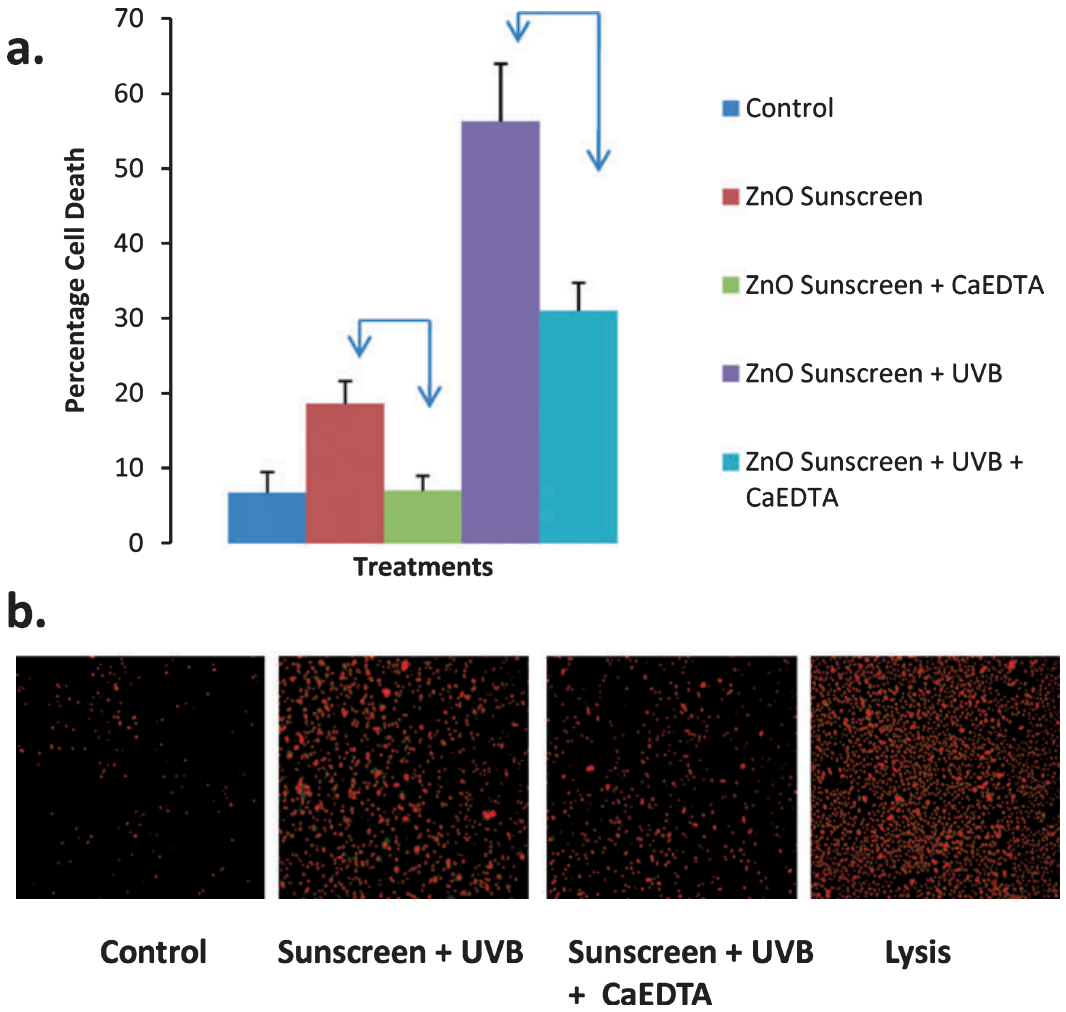

Figure 6 Zinc chelation reduces ZnO sunscreen-induced human epidermal keratinocytes (HEK) death. (a) The histogram shows the percentage of cell death measured with propidium iodide assay in HEK cultures under the following treatments for 5 h: vehicle control, ZnO sunscreen (1 mM), ZnO sunscreen + CaEDTA (1 mM), Zn chelator, UVB-irradiated ZnO sunscreen, UVB-irradiated ZnO sunscreen + CaEDTA. Data are mean ± SE. Insert brackets indicate significant difference $P \geq 0.05$. (b) The representative fluorescent images taken in the following treatments: control, UVB-irradiated ZnO sunscreen, UVB-irradiated ZnO sunscreen + CaEDTA, and lysis with triton X-100.

of inflammatory markers: Interleukin-8 (IL-8), intracellular cell adhesion molecule-1 (ICAM-1), and monocyte chemotactic protein-1 (MCP).[55]

Sunscreens (including those tested in this study) are commonly used products that take advantage of nanotechnology through the incorporation of metal oxides. There is still significant lack of toxicological data for nano-ZnO.[17] Because of the extremely small size of the nanoparticles being used, there is a concern that they may be able to cross cellular membranes and interact directly with macromolecules such as DNA.[12,17,56] A late cytotoxic action of ZnO sunscreen in skin, as suggested in the present study, may be associated with adverse effects when sunscreen users increase time spent in the sun.[6,56,57] The small quantity of Zn^{2+} that accumulates in the space between the sunscreen film and skin may be enough to cause detrimental action and may pose long-term health risks over time. Further studies are needed to understand the exact mechanism behind ZnO-induced cytotoxicity in sunscreen and to examine the effect of Zn^{2+} in a human skin model *in vivo*.

Conflict of Interest

The authors state no conflict of interest.

References

1 Lippens S, Hoste E, Vandenabeele P *et al.* Cell death in the skin. *Apoptosis* 2009; **14**: 549–69.
2 Young C. Solar ultraviolet radiation and skin cancer. *Occup Med (Lond)* 2009; **59**: 82–8.
3 Zhang Q, Southall MD, Mezsick SM *et al.* Epidermal peroxisome proliferator-activated receptor gamma as a target for ultraviolet B radiation. *J Biol Chem* 2005; **280**: 73–9.
4 Gasparro FP. Sunscreens, skin photobiology, and skin cancer: the need for UVA protection and evaluation of efficacy. *Environ Health Perspect* 2000; **108**(Suppl 1): 71–8.
5 FDA. Sunscreen drug products for over-the-counter human use; final monograph. Food and Drug Administration, HHS. Final rule. *Fed Regist* 1999; **64**: 27666–93.
6 Ferrini RL, Perlman M, Hill L. American College of Preventive Medicine practice policy statement: skin protection from ultraviolet light exposure. The American College of Preventive Medicine. *Am J Prev Med* 1998; **14**: 83–6.
7 Hanson KM, Gratton E, Bardeen CJ. Sunscreen enhancement of UV-induced reactive oxygen species in the skin. *Free Radic Biol Med* 2006; **41**: 1205–12.
8 Dufour EK, Kumaravel T, Nohynek GJ *et al.* Clastogenicity, photo-clastogenicity or pseudo-photo-clastogenicity: genotoxic effects of zinc oxide in the dark, in pre-irradiated or simultaneously irradiated Chinese hamster ovary cells. *Mutat Res* 2006; **607**: 215–24.
9 Brunner TJ, Wick P, Manser P *et al. In vitro* cytotoxicity of oxide nanoparticles: comparison to asbestos, silica, and the effect of particle solubility. *Environ Sci Technol* 2006; **40**: 4374–81.
10 George S, Pokhrel S, Xia T *et al.* Use of a rapid cytotoxicity screening approach to engineer a safer zinc oxide nanoparticle through iron doping. *ACS Nano* 2010; **4**: 15–29.
11 Hu X, Cook S, Wang P *et al. In vitro* evaluation of cytotoxicity of engineered metal oxide nanoparticles. *Sci Total Environ* 2009; **407**: 3070–2.
12 Huang CC, Aronstam RS, Chen DR *et al.* Oxidative stress, calcium homeostasis, and altered gene expression in human lung epithelial cells exposed to ZnO nanoparticles. *Toxicol In Vitro* 2010; **24**: 45–55.
13 Palomaki J, Karisola P, Pylkkanen L *et al.* Engineered nanomaterials cause cytotoxicity and activation on mouse antigen presenting cells. *Toxicology* 2009; **267**: 125–31.
14 Reddy KM, Feris K, Bell J *et al.* Selective toxicity of zinc oxide nanoparticles to prokaryotic and eukaryotic systems. *Appl Phys Lett* 2007; **90**: 2139021–3.
15 Bai W, Zhang Z, Tian W *et al.* Toxicity of zinc oxide nanoparticles to zebrafish embryo: a physicochemical study of toxicity mechanism. *J Nanopart Res* 2009; **12**: 1645–1654.
16 Ostrovsky S, Kazimirsky G, Gedanken A *et al.* Selective cytotoxic effect of ZnO nanoparticles on glioma cells. *Nano Res* 2009; **2**: 882–90.
17 Sharma V, Shukla RK, Saxena N *et al.* DNA damaging potential of zinc oxide nanoparticles in human epidermal cells. *Toxicol Lett* 2009; **185**: 211–8.
18 Choi DW, Yokoyama M, Koh J. Zinc neurotoxicity in cortical cell culture. *Neuroscience* 1988; **24**: 67–79.
19 Lobner D, Canzoniero LM, Manzerra P *et al.* Zinc-induced neuronal death in cortical neurons. *Cell Mol Biol (Noisy-le-grand)* 2000; **46**: 797–806.
20 Manev H, Kharlamov E, Uz T *et al.* Characterization of zinc-induced neuronal death in primary cultures of rat cerebellar granule cells. *Exp Neurol* 1997; **146**: 171–8.
21 Stork CJ, Li YV. Rising zinc: a significant cause of ischemic neuronal death in the CA1 region of rat hippocampus. *J Cereb Blood Flow Metab* 2009; **29**: 1399–1408.
22 Yokoyama M, Koh J, Choi DW. Brief exposure to zinc is toxic to cortical neurons. *Neurosci Lett* 1986; **71**: 351–5.
23 Moreira P, Pereira C, Santos MS *et al.* Effect of zinc ions on the cytotoxicity induced by the amyloid beta-peptide. *Antioxid Redox Signal* 2000; **2**: 317–25.
24 Ni ShuilleabhainS, Mothersill C, Sheehan D *et al.* In vitro cytotoxicity testing of three zinc metal salts using established fish cell lines. *Toxicol In Vitro* 2004; **18**: 365–76.
25 Fang F, Futter J, Markwitz A *et al.* UV and humidity sensing properties of ZnO nanorods prepared by the arc discharge method. *Nanotechnology* 2009; **20**: 245502.
26 Liu H, Feng L, Zhai J *et al.* Reversible wettability of a chemical vapor deposition prepared ZnO film between superhydrophobicity and superhydrophilicity. *Langmuir* 2004; **20**: 5659–61.
27 Nagy LN, Abraham N, Sepsi O *et al.* Complex Langmuir-Blodgett films of SiO2 and ZnO nanoparticles with advantageous optical and photocatalytical properties. *Langmuir* 2008; **24**: 12575–80.
28 Nasu A, Otsubo Y. Rheology and UV-protecting properties of complex suspensions of titanium dioxides and zinc oxides. *J Colloid Interface Sci* 2007; **310**: 617–23.
29 Turkoglu M, Yener S. Design and in vivo evaluation of ultrafine inorganic-oxide-containing-sunscreen formulations. *Int J Cosmet Sci* 1997; **19**: 193–201.
30 Domenech J, Prieto A. Stability of ZnO particles in aqueous suspensions under UV illumination. *J Phys Chem* 1986; **90**: 1123–6.
31 McKinlay AF, Diffey BL. A reference action spectrum for ultraviolet-induced erythema in human skin. In: *Human Exposure to Ultraviolet Radiation: Risks and Regulations*. WF Passchier, BF Bosnajakovich, eds. International Congress Series: Elsevier, 1987: 83–87.
32 Tsien R, Pozzan T. Measurement of cytosolic free Ca^{2+} with quin2. *Methods Enzymol* 1989; **172**: 230–62.
33 Linke WF, Seidell A. *Solubilities: Inorganic and Metal-Organic Compounds; A Compilation of Solubility Data from the Periodical Literature*. 4th ed. Washington: American Chemical Society, 1958.
34 Pourbaix M. *Atlas of Electrochemical Equilibria in Aqueous Solutions*. 2d English ed. Houston, TX: National Association of Corrosion Engineers, 1974.

35 Hexsel CL, Bangert SD, Hebert AA *et al.* Current sunscreen issues: 2007 Food and Drug Administration sunscreen labelling recommendations and combination sunscreen/insect repellent products. *J Am Acad Dermatol* 2008; **59**: 316–23.
36 Cheng C, Xin R, Leng Y *et al.* Chemical stability of ZnO nanostructures in simulated physiological environments and its application in determining polar directions. *Inorg Chem* 2008; **47**: 7868–73.
37 Domenech X, Ayllon JA, Peral J. H2O2 formation from photocatalytic processes at the ZnO/water interface. *Environ Sci Pollut Res Int* 2001; **8**: 285–7.
38 Xia T, Kovochich M, Liong M *et al.* Comparison of the mechanism of toxicity of zinc oxide and cerium oxide nanoparticles based on dissolution and oxidative stress properties. *ACS Nano* 2008; **2**: 2121–34.
39 Kasemets K, Ivask A, Dubourguier HC *et al.* Toxicity of nanoparticles of ZnO, CuO and TiO2 to yeast *Saccharomyces cerevisiae*. *Toxicol In Vitro* 2009; **23**: 1116–22.
40 Li Y, Hough CJ, Suh SW *et al.* Rapid translocation of $Zn(^{2+})$ from presynaptic terminals into postsynaptic hippocampal neurons after physiological stimulation. *J Neurophysiol* 2001; **86**: 2597–604.
41 Franklin NM, Rogers NJ, Apte SC *et al.* Comparative toxicity of nanoparticulate ZnO, bulk ZnO, and ZnCl2 to a freshwater microalga (*Pseudokirchneriella subcapitata*): the importance of particle solubility. *Environ Sci Technol* 2007; **41**: 8484–90.
42 Nel A, Xia T, Madler L *et al.* Toxic potential of materials at the nanolevel. *Science* 2006; **311**: 622–7.
43 Frederickson CJ, Koh JY, Bush AI. The neurobiology of zinc in health and disease. *Nat Rev Neurosci* 2005; **6**: 449–462.
44 Kroncke KD. Cellular stress and intracellular zinc dyshomeostasis. *Arch Biochem Biophys* 2007; **463**: 183–7.
45 Mocchegiani E, Malavolta M. Zinc dyshomeostasis, ageing and neurodegeneration: implications of A2M and inflammatory gene polymorphisms. *J Alzheimers Dis* 2007; **12**: 101–9.
46 Hao Q, Maret W. Aldehydes release zinc from proteins. A pathway from oxidative stress/lipid peroxidation to cellular functions of zinc. *FEBS J* 2006; **273**: 4300–10.
47 Wiseman DA, Sharma S, Black SM. Elevated zinc induces endothelial apoptosis via disruption of glutathione metabolism: role of the ADP translocator. *Biometals* 2010; **23**: 19–30.
48 Wiseman DA, Wells SM, Hubbard M *et al.* Alterations in zinc homeostasis underlie endothelial cell death induced by oxidative stress from acute exposure to hydrogen peroxide. *Am J Physiol Lung Cell Mol Physiol* 2007; **292**: L165–77.
49 Jiang D, Sullivan PG, Sensi SL *et al.* $Zn(^{2+})$ induces permeability transition pore opening and release of pro-apoptotic peptides from neuronal mitochondria. *J Biol Chem* 2001; **276**: 47524–9.
50 Gazaryan IG, Krasinskaya IP, Kristal BS *et al.* Zinc irreversibly damages major enzymes of energy production and antioxidant defense prior to mitochondrial permeability transition. *J Biol Chem* 2007; **282**: 24373–80.
51 Bonanni L, Chachar M, Jover-Mengual T *et al.* Zinc-dependent multi-conductance channel activity in mitochondria isolated from ischemic brain. *J Neurosci* 2006; **26**: 6851–62.
52 Dineley KE, Votyakova TV, Reynolds IJ. Zinc inhibition of cellular energy production: implications for mitochondria and neurodegeneration. *J Neurochem* 2003; **85**: 563–70.
53 Bossy-Wetzel E, Talantova MV, Lee WD *et al.* Crosstalk between nitric oxide and zinc pathways to neuronal cell death involving mitochondrial dysfunction and p38-activated K+ channels. *Neuron* 2004; **41**: 351–65.
54 Zhang Y, Aizenman E, DeFranco DB *et al.* Intracellular zinc release, 12-lipoxygenase activation and MAPK dependent neuronal and oligodendroglial death. *Mol Med* 2007; **13**: 350–5.
55 Gojova A, Guo B, Kota RS *et al.* Induction of inflammation in vascular endothelial cells by metal oxide nanoparticles: effect of particle composition. *Environ Health Perspect* 2007; **115**: 403–9.
56 Chiang TM, Sayre RM, Dowdy JC *et al.* Sunscreen ingredients inhibit inducible nitric oxide synthase (iNOS): a possible biochemical explanation for the sunscreen melanoma controversy. *Melanoma Res* 2005; **15**: 3–6.
57 Bigby ME. The end of the sunscreen and melanoma controversy? *Arch Dermatol* 2004; **140**: 745–6.